

Supplementary Materials

Hongmei Hu^{1,2,3*}, Stephan D. Ewert^{2,3}, Birger Kollmeier^{2,3}, Deborah Vickers¹

¹SOUND Lab, Cambridge Hearing Group, Department of Clinical Neuroscience, Cambridge University, Cambridge, UK

²Department of Medical Physics and Acoustics, University of Oldenburg, Oldenburg, Germany

³Cluster of Excellence "Hearing4all", University of Oldenburg, Oldenburg, Germany

Corresponding Author:

Hongmei Hu

Küpkersweg 74, 26129, Oldenburg, Germany

Email address: hh594@cam.ac.uk, hongmei.hu@uol.de

Materials & Methods

Test procedures

Psychoacoustic pretest-experiments

Twelve NH participants (S1 - S12: 6 males and 6 females aged 21- 42 years old, with a mean age of 27.2 years) took part in the psychoacoustic experiment. In the psychoacoustic experiments, the stimuli were generated digitally using a personal computer running MATLAB (The Mathworks, Natick, MA, USA), then converted to analog form using a Fireface UC sound card (RME Audio, Haimhausen, Germany) with 24-bit resolution and a sampling rate of 48 kHz. Then the stimuli were presented to the participants through Sennheiser HD580 headphones at 70 dB sound pressure level (SPL). The participants were seated in a double-walled soundproof booth and responded by clicking the virtual buttons displayed on a monitor.

Three lateralization experiments (5-7 minutes/experiment) were performed to determine the upper frequency limit of left/right discrimination abilities. The experiments used a two-up, one-down, two-alternative forced-choice procedure (2-AFC) to estimate the 71%-correct threshold on the psychometric function (Levitt, 1971). On each trial, two consecutive intervals were presented, separated by 500 ms. Each interval contained four consecutive 400-ms tones or filtered clicks, with 20-ms raised cosine rise/fall ramps, separated by 100 ms. One interval was randomly selected as the standard and had an ITD of the carrier (ITD_{FS}) or ITD of the envelope (ITD_{ENV}) of 0. The other interval, the target, had the same first and third tones as the standard, but the second and fourth tones had a non-zero ITD of the same magnitude as each other. During all three experiments, participants were asked to identify which of the two intervals contained a sequence that appeared to change within the head.

Experiment 1 was conducted to determine the upper limit of the carrier frequency (f_{uplim_c}) for fine structure ITD sensitivity by applying an IPD of $\pi/2$ to the carrier frequency. The experiment utilized SAM tones with a fixed modulation frequency (f_m) of 40 Hz and an adaptive carrier

41 frequency (f_c) ranging from 100 Hz to 4000 Hz. The carrier frequency was adjusted using
 42 adaptation factors of 1.4, 1.2, and 1.1, starting at 1000 Hz. Before the formal experiment, a brief
 43 training task was provided to familiarize the participants with the procedures. After eight
 44 reversals, the formal test was terminated and the threshold was calculated as the geometric
 45 mean of the last six reversal values. This procedure was adapted from the binaural TFS
 46 sensitivity test (TFS-AF) (Füllgrabe et al., 2017; Füllgrabe and Moore, 2017).
 47 Experiment 2 was conducted to determine the upper limit of the modulation rate (f_{uplim_m}) for
 48 envelope ITD sensitivity, with a fixed ITD of 500 μ s (dichotic) or 0 (diotic) applied to the
 49 envelope. The f_c was fixed at 4000 Hz, while the f_m was adaptive. Experiment 3 was performed
 50 to determine the upper limit of the pulse rate (f_{uplim_pps}) for interaural pulse time difference
 51 (IPTD) sensitivity, using an ITD of 500 μ s applied to pulses and adjusting the pulse rate. Both
 52 experiments were similar to experiment 1, except that in experiments 2 and 3, the start f_m or
 53 pulse rate was 100 Hz or 100 pps, with a minimum and maximum of 10 Hz or pps and 1500 Hz
 54 or pps, respectively. The adaptation factors were 80, 40, and 20. To accommodate individual
 55 differences, an upper limit for the adaptive f_m was not set. This may have resulted in some
 56 participants perceiving lower sidebands of the modulation as audible for higher modulation rates
 57 (e.g., above \sim 350 Hz) (Kohlrausch et al., 2000), transforming the ITD change detection task into
 58 a disparity detection task not only based on envelope ITD cues. The decision not to set an
 59 upper limit was made to consider the possibility that participants may use other cues, which
 60 could also trigger ACC responses.

61 *Stimuli*

62 *SAM tones*

63 In both experiments 1 and 2, SAM tones were generated digitally according to equation (1)
 64 (Bernstein and Trahiotis, 2012; Hu et al., 2022).

$$s(t) = a \sin(2\pi f_c t)(1 - \cos 2\pi f_m t) \quad (1)$$

65 Figure 3A, column 1, shows an example of a stimulus used in the psychoacoustic experiment 1
 66 (SAM tones ITD_{FS} , $f_c = 1000$ Hz and $f_m = 40$ Hz). In this example, the first interval is the target
 67 (row 2), and the second interval is the standard (row 3). Both the psychoacoustic and EEG
 68 experiments employed IPD of 0 or $\pi/2$. EEG experiment 1 tested four carrier frequencies, $f_c =$
 69 [400, 800, 1200, 1600] Hz. Figure 3B, column 1, shows an example of a stimulus used in EEG
 70 experiment 1 (SAM tones ITD_{FS} , $f_c = 400$ Hz and $f_m = 40$ Hz), where each presentation lasted 8
 71 seconds (s). The sequence included 2 s of the diotic stimulus (IPD = 0 in time window T1),
 72 followed by 2 s of the dichotic stimulus (IPD = $\pi/2$ in time window T2; T1 \rightarrow T2 referred to as
 73 outward switching), then 2 s of the standard stimulus (IPD = 0 in time window T3; T2 \rightarrow T3
 74 referred to as inward switching), and 2 s of silence (in time window T4).

75 The stimuli used in the second psychoacoustic experiment (not shown in Figure 3A) were also
 76 SAM tones, but the ITD was applied to the envelope instead of the carrier. In EEG experiment
 77 2, four modulation frequencies were tested $f_m = [40, 80, 160, 320]$ Hz. Figure 3B, column 2
 78 shows an example of a stimulus used in this experiment (SAM tones ITD_{ENV} , $f_c = 4000$ Hz and
 79 $f_m = 40$ Hz). Like in EEG experiment 1, it consisted of 2 s of the diotic stimulus ($ITD_{ENV} = 0$ in
 80 the time window T1), followed by 2 s of the dichotic stimulus ($ITD_{ENV} = 500$ μ s in the time

81 window T2; with an outward switching T1→T2), then again 2 s of the standard stimulus
82 (ITD_{ENV} = 0 in the time window T3; with an inward switching T2→T3), and 2 s of silence (in the
83 time window T4). As Ross (2018) showed no detectable ACCs in most of their participants for
84 the 4000 Hz SAM, the ACCs in experiment 2 might be smaller than in experiment 1 or absent.

85 Note that, as in (Kohlrausch et al., 2000), no precautions were taken to mask possible distortion
86 products in both psychoacoustic and the EEG experiment 2.

87 *Filtered clicks*

88 In experiment 3, filtered clicks generated as in (Hu et al., 2017; Hu et al., 2022) were used to
89 simulate the signal delivered to CI users. The pulse train was band-limited to 3-5 kHz with a
90 center frequency of $f_c = 4$ kHz. These band-limited pulse trains $p(t)$ were then sinusoidally
91 amplitude-modulated using formula (2).

$$92 \quad s(t) = p(t) * [1 - \cos(2\pi * f_m * t)] \quad (2)$$

93 The f_m in the psychoacoustic was 2.5 Hz (reciprocal of the duration of consecutive filtered
94 clicks, i.e. 1/0.4s), while it was 10 Hz in EEG experiments. This type of SAM ensures that stimuli
95 start at the trough of the modulation.

96 Figure 3A (column 2) and B (column 3) show an example of the stimuli used in the
97 psychoacoustic (filtered clicks IPTD, pulse rate = 160 pps and $f_m = 2.5$ Hz, IPTD = 0 or IPTD =
98 500 μ s) and EEG experiments (filtered clicks IPTD, pulse rate = 160 pps and $f_m = 10$ Hz, IPTD =
99 0 or IPTD = 500 μ s), respectively. In the EEG experiment, four fixed pulse rates of [40, 80, 160,
100 320] pps were used. The duration of each presentation is 6 s, which includes 2 s of the diotic
101 stimulus, followed by 2 s of the dichotic stimulus (with a transition from T1→T2, referred as
102 outward switching), and 2 s of silence (in time window T4, with a T2→T3 inward switching).

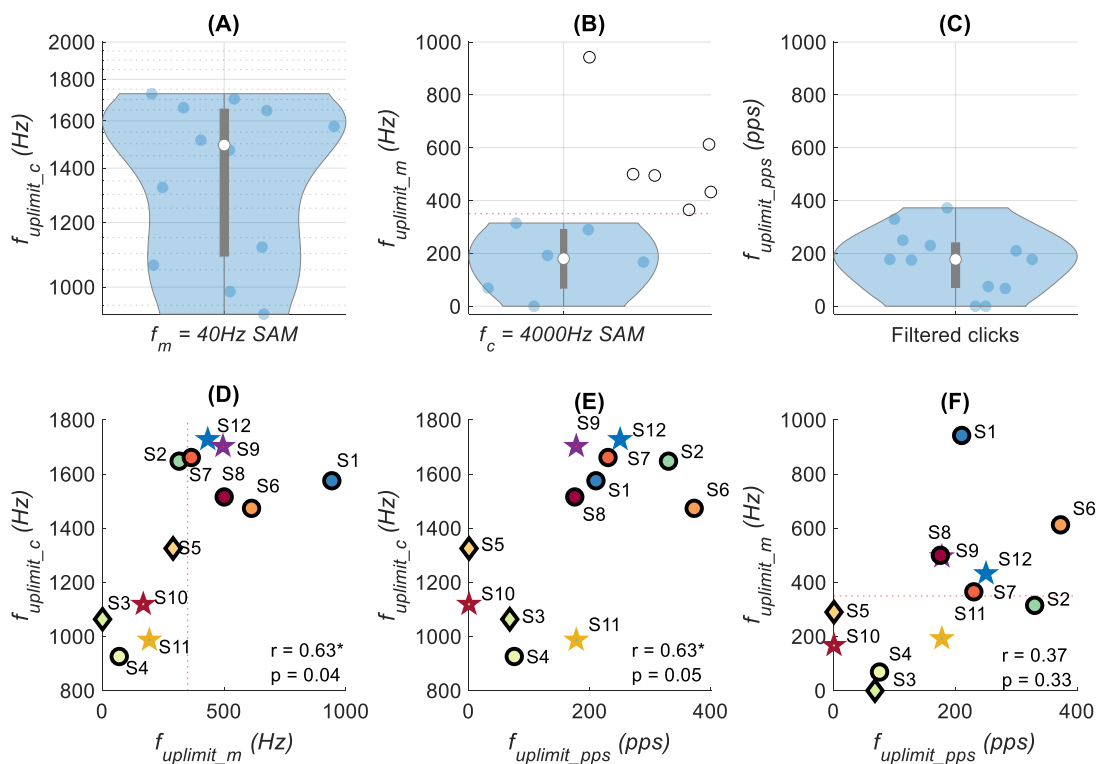
103 In both the psychoacoustics and EEG experiment 3, a low-pass noise, uncorrelated between
104 the ears, was added to the filtered clicks to conceal potential distortion products. The low-pass
105 noise was created by generating broadband noise in the time domain, converting it to the
106 frequency domain, and setting the power of all components above 1000 Hz to zero. The noise
107 was then manipulated to have a flat spectrum up to 200 Hz with a decreasing spectral density of
108 3 dB/octave above 200 Hz. It was further filtered with a 5th-order, lowpass filter with a cut-off
109 frequency of 1000 Hz (Hu et al., 2017), and gated with 50-ms raised cosine ramps. The test
110 stimulus was centered within the noise presentation, which was presented at 40 dB SPL.

111 We chose 4000 Hz instead of a higher carrier frequency such as 8000 Hz for several reasons:
112 Firstly, Previous studies have shown that the upper modulation rate is lower for stimuli centered
113 at 8000 Hz compared to those centered at 4000 Hz (Bernstein and Trahiotis, 2013). Since only
114 2 out of 14 participants in Ross (2018) showed significant responses at 4000 Hz, we would
115 expect similar or even smaller responses at 8000 Hz. Secondly, as the aging population is one
116 target group for future studies, high-frequency hearing loss may make a higher frequency less
117 optimal. Lastly, although it is not a critical factor, 8000 Hz is less pleasant to listen to than 4000
118 Hz.

119 **Results**

120 *Psychoacoustic pretest results*

121 Supplementary Figure 1 shows the violin plots of the f_{uplim_c} , f_{uplim_m} , and f_{uplim_pps} from three
 122 psychoacoustic experiments. The violin plots (Hintze and Nelson, 1998) were generated using
 123 freely available Matlab code (<https://github.com/bastibe/Violinplot-Matlab>). The original box plot
 124 shape is included as a grey box in the center of the violin. Supplementary Figure 1 depicts the
 125 individual data of the 12 participants as solid blue dots that have been randomly jittered from the
 126 center. The corresponding density curves have been constructed around each center line. If the
 127 participant couldn't do the task, the value was set to 0.123456. Supplementary Figure 1
 128 indicates that the upper limits vary across participants. The mean and standard deviation of
 129 f_{uplim_c} is 1393 ± 284 Hz, which is in the range of previously reported values (Ross et al.,
 130 2007a; Ross et al., 2007b; Grose and Mamo, 2010; Hopkins and Moore, 2010, 2011; Brughera
 131 et al., 2013; Füllgrabe and Moore, 2017; Papesh et al., 2017; Füllgrabe and Moore, 2018). It
 132 should be noted that the top-performing participant in this study exhibited a higher f_{uplim_c} than
 133 those reported in (Klug and Dietz, 2022), possibly due to the utilization of different stimuli and
 134 test procedures. The purpose of the pretests is to select the rate conditions for in the EEG
 135 experiments. The exactly upper frequency limit in humans is not the focus of this study, and
 136 more detailed discussions are beyond the scope of this paper.



137 Supplementary Figure 1 the top panels of the figure show violin plots of the upper limit frequency f_c obtained from the psychoacoustic
 138 experiment for each participant, represented by solid dots in each violin plot. The bottom panels display the correlation between the three
 139 upper limit frequencies. Participants S9-S12 (represented by pentagram symbols) were unable to attend the EEG experiment, while S3 couldn't
 140 achieve f_{uplim_m} and S5 couldn't achieve f_{uplim_pps} , represented by diamond symbols. The dotted red lines in panels B, D, and F indicate the
 141 boundary of 350 Hz.
 142

143 The top middle panel of Supplementary Figure 1 shows the f_{uplim_m} . Without setting a limit in
 144 the adaptive procedure, some participants reached f_{uplim_m} above 350 Hz. Participant S1 even
 145 reached 980 Hz. This was expected because the task may become easier again for some

146 participants if they are able to use spectrally resolve sidebands at modulation rates above a
147 certain frequency (e.g., ~ 350 Hz, the red dotted horizontal line) (Kohlrausch et al., 2000). This
148 phenomenon may be more prominent in the disparity detection test procedure used in this
149 study, compared to the classical left/right discrimination tasks. To avoid misleading
150 interpretation, the mean and standard deviation of f_{uplim_m} were calculated after excluding data
151 from participants who couldn't complete the task (S3) and those with f_{uplim_m} above 350 Hz (6
152 data points as indicated by the empty circles in the upper middle panel of Supplementary Figure
153 1, which may be a result of the resolved sidebands). The resulting mean and standard deviation
154 were 207 ± 99 Hz. Some caution is necessary when interpreting the correlation between the
155 f_{uplim_m} and other experimental results. However, the same issue was not apparent for the EEG
156 results shown in Section 3.2, because the maximum modulation frequency tested in the EEG
157 experiment was limited to 320 Hz. The mean and standard deviation of f_{uplim_pps} for filtered
158 clicks, after excluding S5 and S10, were 207 ± 97 pps. The Pearson correlation coefficients
159 between the three upper limits are as follows: between f_{uplim_c} and f_{uplim_m} (exclude S3), $r =$
160 0.63 , $p = 0.04$; between f_{uplim_c} and f_{uplim_pps} (excluded S5 and S10), $r = 0.63$, $p = 0.05$; and
161 between f_{uplim_m} and f_{uplim_pps} (excluded S3, S5, and S10), $r = 0.37$, $p = 0.33$.
162 S3 and S5 were unable to perform the corresponding experiments. However, both detected
163 changes when presented with 100 Hz SAM tones and 100 pps filtered clicks with 500 μ s ITD. It
164 was speculated that this was mainly due to the large initial adaptive stepsize and their difficulty
165 in focusing during the first reversal. S8 reported that he occasionally experienced mild tinnitus.
166 Despite this, he was included in the EEG experiment as his audiometry results were within
167 normal hearing range and his lateralization performance was above average. Regrettably,
168 participants S9-S12 were unable to attend the EEG experiments due to reasons relating to the
169 COVID-19 pandemic.

170 *Additional EEG results*

171 *Time domain (CAEPs)*

172 ■ CAEPs of experiment 1

173 Regarding experiment 1 (ITD_{FS} , page Figure 4A and Figure 6A), the amplitude and latency of
174 the offset responses (aqua) were relatively consistent across different carrier frequencies and
175 the N1 latency of the offset responses was generally shorter compared to the onset and ACC
176 responses.

177 The N1P2 amplitude was significantly affected by carrier frequency (f_c), response type, and
178 their interaction according to GLMrm ($p < 0.005$). The mean amplitude was
179 $7.318/6.063/5.094/4.023$ μ V for 400/800/1200/1600 Hz, respectively. There were no significant
180 differences between 400, 800, and 1200 Hz, but the N1P2 amplitude for the 1600 Hz was
181 significantly smaller than the other carrier frequencies. For the offset CAEPs, there were no
182 significant differences between carrier frequencies. For most of the onset CAEPs, the
183 differences were not significant except that the N1P2 amplitude of 1200 Hz was slightly larger
184 than that of 1600 Hz ($p = 0.048$). For ACC1 (outward) responses, the N1P2 amplitudes of 400

185 Hz and 800 Hz were significantly larger than the 1200 and 1600 Hz, but there were no
186 significant differences between 400 and 800 Hz, and between 1200 Hz and 1600 Hz. For ACC2
187 (inward) responses, the N1P2 amplitude of 800 Hz was significant larger than that of 1200 and
188 1600 Hz, and the N1P2 amplitude of 400 Hz was significantly larger than that of 1600 Hz.

189 The mean N1P2 amplitudes were 8.577/4.816/4.172/4.932 μV for onset/ACC1/ACC2/offset
190 responses, respectively. The onset CAEPs were significantly larger than the ACC1, ACC2, and
191 offset CAEPs. However, there were no significant differences between the three latter types.
192 Pairwise comparisons within each f_c showed that the onset CAEPs were significantly larger than
193 the offset CAEPs only for 400 and 1200 Hz. There were no significant differences between
194 ACC1 and ACC2 for all carrier frequencies. Significant correlations were observed between the
195 onset N1P2 amplitudes of most carrier frequencies, except for 400 vs 1200 Hz, and 400 vs
196 1600 Hz.

197 The mean N1 latency was 114/132/137/95 ms for onset/ACC1/ACC2/offset, respectively. The
198 GLMrm analysis showed a significant effect of response type ($p < 0.001$), but no significant effect
199 of f_c and their interaction. Pairwise comparisons showed significant differences between most
200 response types ($p < 0.01$), except between ACC1 and ACC2. The N1 latency of ACC responses
201 was significantly larger than the onset response, while the offset response had the shortest
202 latency and was significantly smaller than the other response types.

203 In summary, the results from experiment 1 were generally consistent with Ross et al. (2007b).
204 For example, the mean P1, N1, and P2 amplitudes of ACC were smaller than those of the onset
205 response: P1, 1.684/1.405/1.005/0.248 μV ; N1, 3.324/-1.299/-1.019/-2.146 μV ; P2,
206 3.946/2.128/1.862/2.379 μV for onset/acc1/acc2/offset. The ACC latencies were delayed
207 compared with the corresponding onset and offset ones: P1, 42/46/57/27 ms; N1,
208 114/132/137/95 ms; P2, 211/227/240/213 ms for the onset/ACC1/ACC2/offset. The mean
209 latencies of both P1 and N1 were in the same range but slightly smaller than Ross et al.
210 (2007a). The latencies of ITD_{FS} change evoked ACC1 and ACC2 that were longer than the
211 onset, and the differences were smaller than Ross et al. (2007a). Consistent with (Ross, 2018),
212 there was a tendency for larger responses to outward IPD changes (ACC1) than inward
213 changes (ACC2) for the lower carrier frequencies, however, it was not significant here ($p > 0.5$).

214

215 ■ CAEPs of experiment 2

216 In experiment 2 (ITD_{ENV}), as demonstrated in paper Figure 4B and Figure 6B, similar to
217 experiment 1, there were clear onset and offset responses in all four test conditions. The onset
218 N1P2 amplitude was comparatively larger than the offset responses, but the difference between
219 the onset and offset CAEPs was smaller compared to those shown in paper Figure 4A and
220 Figure 6A. Consistent with the findings of Ross (2018), the N1P2 amplitudes of both onset and
221 offset CAEPs were larger than the ACC responses, due to the tiny (close to the noise floor) or
222 absence of ACC responses.

223 Regarding the N1P2 amplitude in experiment 2, a GLMrm analysis revealed significant effects
224 of f_m , response type, and their interaction. The mean amplitude was 4.249/4.228/5.258/5.665
225 μV for f_m of 40/80/160/320 Hz, respectively. A significant difference between f_m was only
226 observed for 80 Hz vs 160 Hz. Consistent with this, pairwise comparisons within each response
227 type only showed a just significant smaller onset N1P2 amplitude in 80 Hz condition compared

228 to the 160 Hz condition ($p = 0.048$). The mean amplitude was 8.547/2.543/1.853/6.458 μV for
229 onset/ACC1/ACC2/offset, respectively. Both onset and offset CAEPs were larger than the ACC
230 responses. There were no significant differences between ACC1 and ACC2, and between onset
231 and offset. Within each f_m , pairwise comparisons also showed no significant difference between
232 onset and offset CAEPs, and between ACC1 and ACC2 responses (near noise floor). The onset
233 and offset CAEPs were significantly larger than ACC responses, except for the comparison
234 between ACC1 and offset for $f_m = 80$ Hz, and between ACC1 and offset, and ACC2 and offset
235 for $f_m = 160$ Hz. Significant correlations were observed among modulation frequencies for all
236 onset N1P2 amplitudes and for most offset N1P2 amplitudes, except for 320 vs 40, and 320 vs
237 160 Hz. The offset CAEPs were more correlated with the ACC responses than with the onset
238 responses, mainly due to their small amplitudes.

239 For N1 latency, the GLMrm analysis showed no significant effect of either f_m or response type.
240 The mean latency was 107/109/107/101 ms for onset/ACC1/ACC2/offset, and 107/105/104/109
241 ms for 40/80/160/320 Hz.

242

243 ■ CAEPs of experiment 3

244 Regarding the filtered clicks (paper Figure 4C and Figure 6C), there were no ACC2 responses
245 (for inward IPTD changes) recorded in experiment 3. Overall, the N1P2 amplitude of both onset
246 and offset responses increased with increasing pulse rates. Similarly to experiment 2, the ACC1
247 responses were either small (near the noise floor) or absent.

248 For N1P2 amplitude, GLMrm showed a significant effect of pulse rate, response type, and their
249 interactions ($p < 0.01$). The mean amplitude was 2.31/3.43/5.36/5.35 μV for 40/80/160/320 pps,
250 respectively. There were no significant differences between pulse rates of 40 and 80 pps, and
251 between 160 and 320 pps. Within each response type, pairwise comparisons showed no
252 significant differences between pulse rates for both ACC1 and offset responses. For the onset
253 CAEPs, there were significant differences between most pulse rates ($p < 0.01$), except for
254 conditions of 40 vs 80 pps, and 160 vs 320 pps. The mean amplitude was 5.48/2.52/4.34 μV for
255 onset/ACC1/offset, and only the difference between onset and ACC1 responses was significant.
256 Within each pulse rate, pairwise comparisons showed no significant differences between
257 response types for most pulse rates, except that for 160 pps and 320 pps, there was a
258 significantly larger onset N1P2 amplitude than the offset one ($p = 0.009$, and $p = 0.014$). There
259 were no correlations between N1P2 amplitudes of different pulse rates for both onset and offset
260 responses.

261 For N1 latency, GLMrm revealed a significant effect of pulse rate, but not of response types or
262 their interactions. The mean latency was 141/134/119/114 ms for 40/80/160/320 pps,
263 respectively. The N1 latency was significantly shorter for 320 pps compared to 40 pps and 80
264 pps, and for 160 pps compared to 80 pps. Within each response type, pairwise comparison
265 showed significant N1 latency differences only for 320 pps vs 40 pps, 320 pps vs 80, and 80
266 pps vs 160 pps for the onset CAEPs, and between 40 pps and 320 pps ($p = 0.044$) for ACC1.
267 The mean latency was 131/129/120 ms for onset/ACC1/offset responses with no significant
268 differences between them. Within each pulse rate, there were nearly no significant differences
269 between the three response types, except that the onset N1 latency was significantly larger than
270 the offset one ($p = 0.011$) for the 80 pps.

271 ▪ Comparison CAEPs evoked with 40 Hz modulation rate stimuli

272 In experiment 3, we did not measure ACC2 data (inwards changes) for the filtered clicks, so
273 only the onset, ACC1 (outwards changes), and offset responses of the five types of 40 Hz
274 modulated SAM tones and the 40-pps filtered clicks were analyzed using GLMrm (with factors:
275 stimuli type [400/800/1200/1600/4000SAM/40-pps-clicks], and response type [onset, ACC1 and
276 offset]).

277 GLMrm showed a significant effect ($p < 0.005$) of stimulus type, response type, and their
278 interaction on the N1P2 amplitude. The mean amplitude was
279 7.544/6.271/5.860/4.759/5.046/2.309 μV for 400/800/1200/1600/4000SAM/40-pps-clicks,
280 respectively. Pairwise comparison revealed significant differences between 400 Hz and 1600 Hz
281 SAM tones, and between 40-pps filtered clicks and all four low-frequency SAM tones. Within
282 each response type, the pairwise comparison showed that: 1) the onset response amplitude of
283 the 40-pps filtered clicks was significantly smaller than most SAM tones except for the 800 Hz;
284 2) the 400 and 800 Hz SAM tones evoked significant larger responses than the other three SAM
285 tones and the 40-pps filtered clicks for ACC1 response; 3) there were no significant differences
286 among different stimulus types for the offset responses.

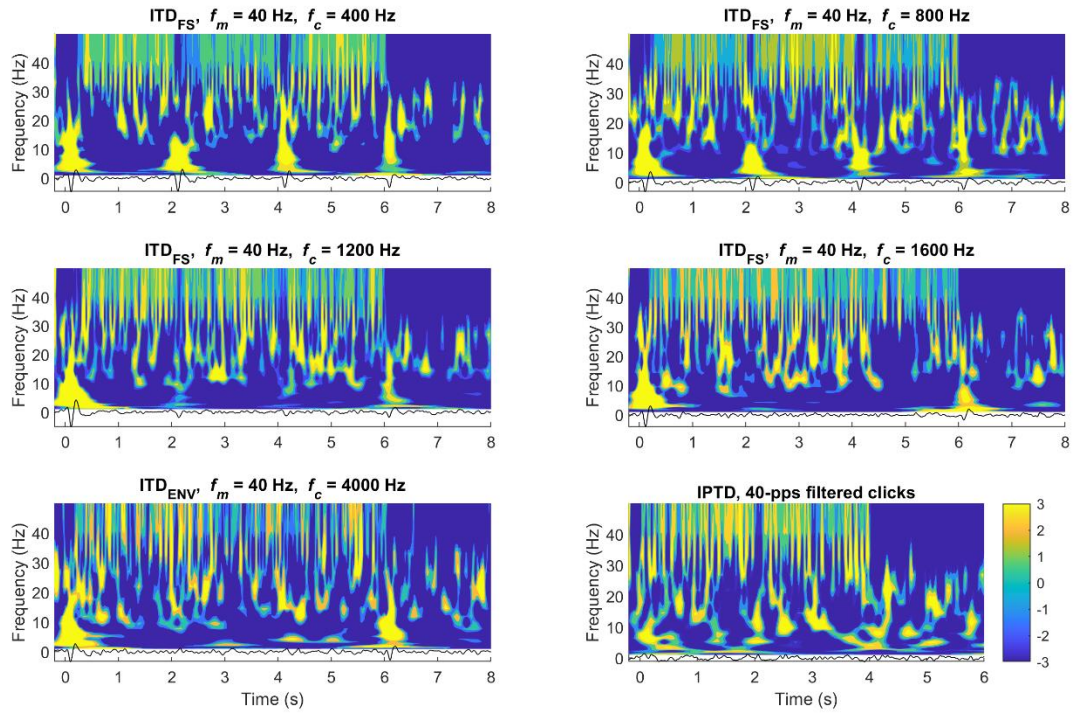
287 The GLMrm analysis revealed a significant effect of stimulus type, response type, as well as
288 their interaction on N1 latency. The mean latency was 110/112/114/120/104/141ms for
289 400/800/1200/1600/4000SAM/40-pps-clicks. Pairwise comparison showed significant
290 differences in latency between 1600 Hz and 4000 Hz SAM tones, and between 40-pps filtered
291 clicks and the four low-frequency SAM tones. Further analysis within each response type
292 showed that for onset responses, the 40-pps filtered clicks had a significantly different latency
293 from most other stimulus types, except for the 1600 Hz SAM tones ($p = 0.051$). Within each
294 stimulus type, there were no significant differences in latency among the three response types
295 for both 4000 Hz SAM tones and 40-pps filtered clicks.

296

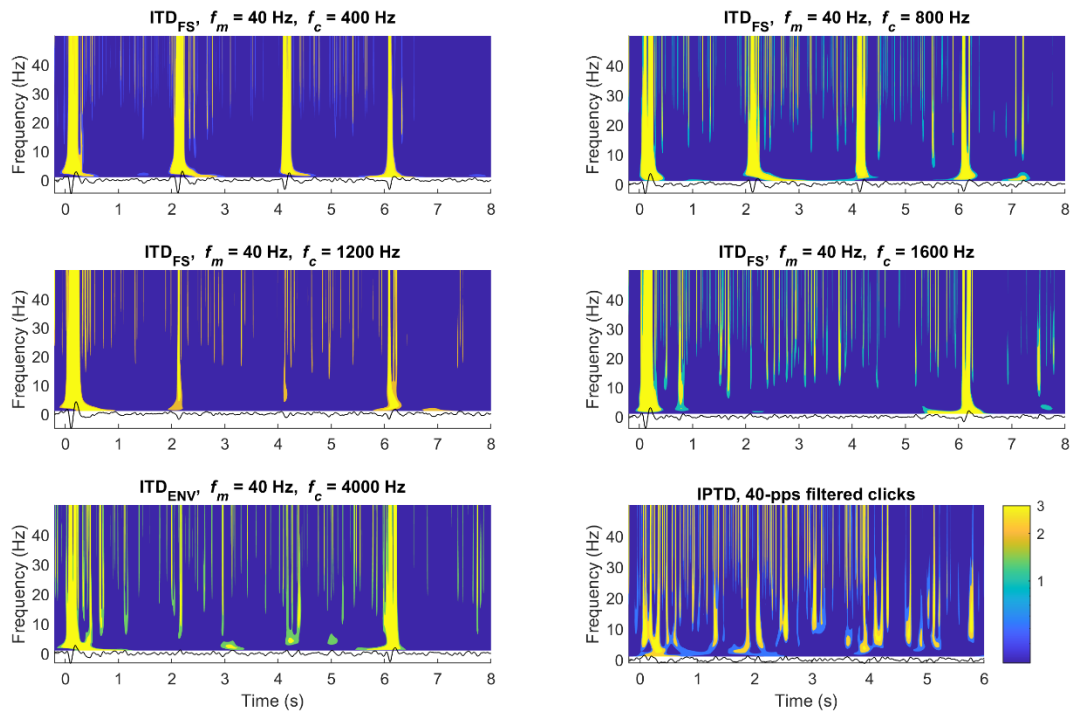
297 *Time-frequency domain*

298 Supplementary Figure 2A shows the time-frequency representations or wavelet spectrograms
299 after wavelet transformations for stimuli with 40-Hz modulation frequency or 40-pps pulse rate in
300 the frequency range of 2-50 Hz in the linear y-scale. The wavelet spectrograms reveal that the
301 onset, ACC1, ACC2, and offset CAEPs are primarily dominated by frequencies below 30 Hz,
302 while the 40-Hz ASSRs are centered around 40 Hz except during the 2s-silence period. Wavelet
303 time-frequency visualization reveals some interactions between the transient CAEPs and
304 ASSRs. A clear reset, represented by blue gaps in the 40 Hz regions, can be seen in the
305 ASSRs whenever the P1-N1-P2 complex is detected and pronounced. This suggests that the
306 transient CAEPs desynchronize the steady-state activity. For example, for f_c of 400, 800, and
307 1200 Hz, the ASSRs were suppressed or reset at approximately 0, 2, and 4 s, respectively, and
308 the ASSRs in these time windows (T1, T2, T3) exhibit notable energy differences.

309
310



(A)



(B)

311

312

313

314

315

Supplementary Figure 2 The average response in the time-frequency domain for conditions with $f_m = 40$ Hz or pulse rate = 40 pps. (A) the number of cycles is $n = 6$, and (B) $n = 2$, with log colorscale. The time-frequency spectrum was obtained by applying wavelet analysis on the average response shown at the bottom of each panel.

316 Both Figure 8 and Supplementary Figure 2A have $n = 6$ cycles, which determines the temporal
317 and spectral precision. An increase in n leads to decreased temporal precision but increased
318 spectral precision, and vice versa. To prioritize temporal precision, Supplementary Figure 2B
319 presents the same results as Supplementary Figure 2A but with $n = 2$ cycles. The color bar
320 uses a log color scale for improved visualization. Compared to the ACC evoked by low-
321 frequency ITDfs, Supplementary Figure 2B shows that the change responses evoked by the
322 high-frequency ITDenv are much smaller and more similar to the surrounding brain activities,
323 making it more challenging to determine the presence of ACC response.

324 *Frequency domain (ASSRs)*

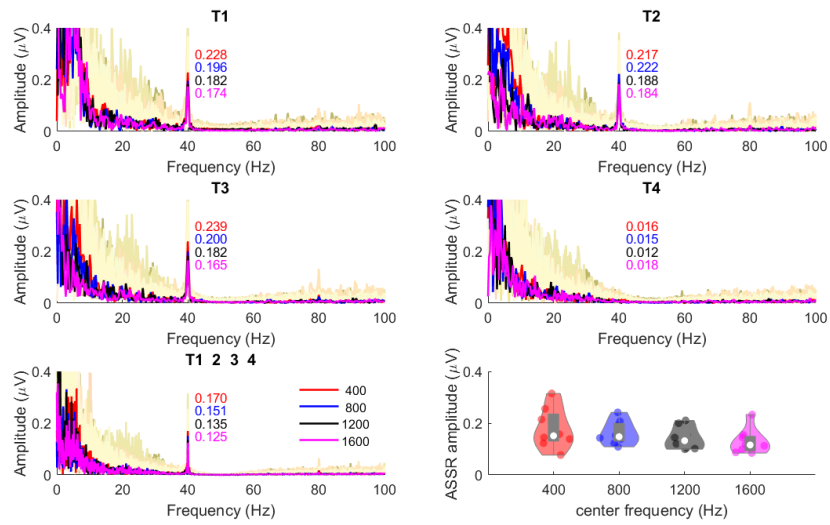
325 A comparison between the 40-Hz ASSRs shown in Supplementary Figure 3 (A, the top-left
326 panel of B and C, with the two parallel red dashed lines representing 30 and 50 Hz,
327 respectively) and Supplementary Figure 2 reveals slight differences in different time durations.
328 To examine possible differences in the steady state responses before and after interruption by
329 the stimulus onset, ITD changes, and offset, the ASSRs in different time windows were
330 analyzed.

331 Supplementary Figure 3 shows the overall average ASSRs across participants for different
332 analysis windows (panels 1-5: T1, T2, T3, T4, T1234, or T124). The colored curves in the cream
333 area are the average ASSR from each individual. The red, blue, black, and pink curves
334 represent the group average ASSR across participants for various test conditions: (A) $f_c = [400,$
335 $800, 1200, 1600]$ Hz; (B) $f_m = [40, 80, 160, 320]$ Hz; (C) pulse rate = $[40, 80, 160, 320]$ pps. The
336 numbers with corresponding colors indicate the ASSR values at the modulation frequency within
337 one of the analysis windows. The bottom right panel shows violin plots of the ASSR amplitude
338 at the modulation frequency, within 8s (T1234) for the SAM tones or 6s (T124) for the filtered
339 clicks.

340 In general, the 40-Hz ASSR decreased with increasing carrier frequency for the SAM tones.
341 There was no ASSR in T4 (silence), the values shown are the noise floor around the modulation
342 frequency, as expected.

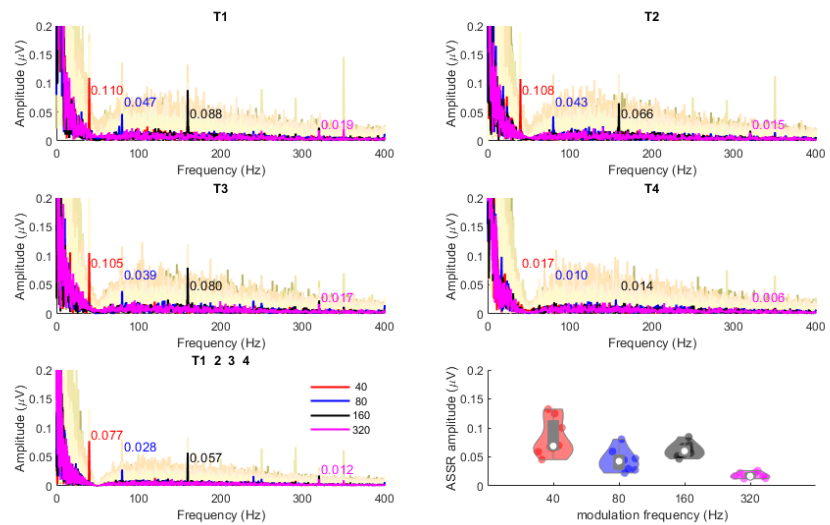
343 Regarding experiment 1 (Supplementary Figure 3A), the overall mean 40-Hz ASSR amplitudes
344 were 0.206/0.215/0.209/0.035/0.153 μ V within T1/T2/T3/T4/T1234, and 0.187/0.173/0.152/0.142
345 μ V for 400/800/1200/1600 Hz. As found by Ross (2018), the amplitude of the 40-Hz ASSR
346 within T1234 declined gradually with increasing carrier frequency. GLMrm (factors: analysis
347 window, T1, T2, T3, T4, T1234; f_c) showed significant effect of f_c and analysis window, as well
348 as their interaction. However, pairwise comparison showed no significant differences between
349 different carrier frequencies. Pairwise comparison revealed significant differences between T4
350 (silence) and the other analysis windows (T1, T2, T3, T1234), as well as between T1234 and
351 the other windows (T1, T2, T3, T4). Within each carrier frequency, the 40-Hz ASSR amplitudes
352 were not significantly different among T1, T1, and T3.

353 The 40-Hz ASSR of different f_c SAM tones were all correlated, but there was no correlation
354 between the f_c limit and either N1P2 or 40-Hz ASSR amplitude.



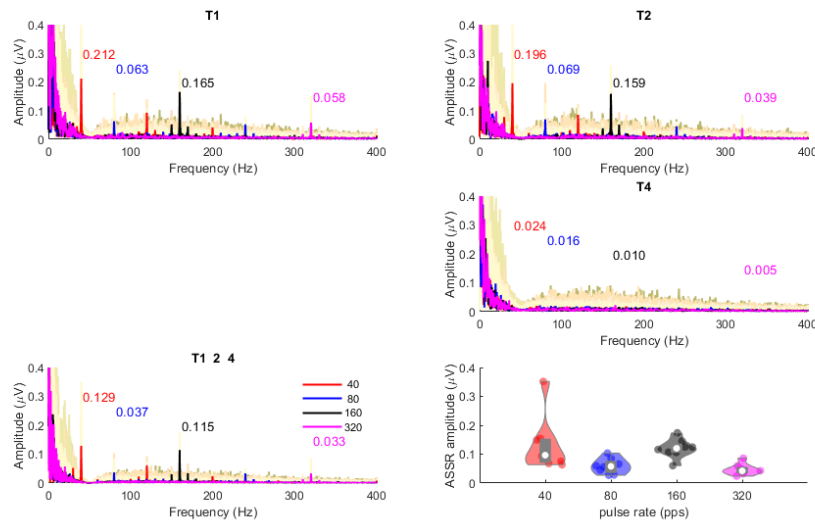
355

(A)



356

(B)



(C)

357

358 Supplementary Figure 3 The individual and group average ASSRs in the frequency domain. The red, blue, black, and pink spectrums are the
 359 overall average ASSR across participants for different test conditions: (A) $f_c = [400, 800, 1200, 1600]$ Hz;. (B) $f_m = [40, 80, 160, 320]$ Hz;. (C) pulse
 360 rate = $[40, 80, 160, 320]$ pps. All the other colored curves in the background are the average ASSR from each individual. The first five panels are
 361 the ASSRs in different analysis time windows (T1, T2, T3, T4, T1234, or T124). The numbers shown in different colors are the 40-Hz ASSR values
 362 within the corresponding time window for each carrier frequency. The bottom right panel shows the violin plots of the ASSR amplitude for each
 363 carrier frequency, with an analysis window of 8s (T1234) for SAM tones or 6s (T124) for the filtered clicks. The solid dots in each violin plot are
 364 individual ASSRs at the corresponding f_m or pulse rate of each participant.

365 Supplementary Figure 3B and C show the ASSRs at modulation rates of 40, 80, 160, and 320
 366 Hz in various analysis time windows. The values in different colors indicate the corresponding
 367 ASSR values at different modulation rates. In general, the ASSRs of high carrier frequency
 368 stimuli are smaller than those of low carrier frequency (≤ 1600) SAM tones, and the ASSRs of
 369 filtered clicks are larger than those of high carrier frequency SAM tones. Among both types of
 370 high-frequency stimuli, the order is 40-Hz ASSR > 160-Hz ASSR > 80-Hz ASSR > 320-Hz
 371 ASSR. The larger 40-Hz ASSR evoked by the filtered clicks is mainly due to better phase
 372 locking to the envelope, as reported by Hu et al (2022).

373 Regarding experiment 2 (Supplementary Figure 3B), the overall mean ASSR amplitudes were
 374 0.079/0.071/0.072/0.033/0.052 μV within T1/T2/T3/T4/T1234, and 0.093/0.058/0.071/0.022 μV
 375 for 40/80/160/320 Hz. GLMrm (factors: analysis window, T1, T2, T3, T4, T1234; f_m) showed
 376 significant effect of f_m and analysis window, as well as their interaction. Pairwise comparisons
 377 showed no significant differences for f_m 40 vs 80, 40 vs 160, 80 vs 160 Hz. Similar to
 378 experiment 1, pairwise comparisons showed significant differences between T4 (silence) and
 379 the other analysis windows (T1, T2, T3, T1234) as well as between T1234 and the other four
 380 analysis windows, both across modulation frequencies and within individual ones. Pairwise
 381 comparisons for each analysis window showed that within T1, there were significant differences
 382 between most pulse rates except for 40 vs 160, 80 vs 160 pps; for T2, T3, T4, and T1234, the
 383 ASSR of 320 Hz was significantly smaller (T2, $p < 0.01$; T3, T4, and T1234, $p < 0.05$) than the
 384 other three modulation frequencies. There was no correlation between the f_m limit and the
 385 N1P2 amplitude or the ASSR amplitude. The onset responses of different modulation
 386 frequencies were all correlated with each other, and the offset N1P2 amplitudes of 40, 80, and
 387 160 Hz were correlated with each other, but not with that of 320 Hz.

388 For experiment 3 (Supplementary Figure 3C), the mean ASSR amplitudes were
389 0.143/0.131/0.032/0.089 μV in T1/T2/T4/T124, and 0.148/0.075/0.123/0.048 μV for
390 40/80/160/320 pps. GLMrm (factors: analysis window, T1, T2, T4, T124; f_m) showed significant
391 effect of f_m and analysis window, as well as their interaction. Pairwise comparison only showed
392 significant ASSR amplitude differences for 160 vs 80, and 160 vs 320 pps. Unlike experiments 1
393 and 2, the pairwise comparison showed significant differences among all the analysis windows.
394 Specifically, the 160 pps condition evoked a significantly larger ASSR compared to the 80 and
395 320 pps conditions within both T1 and T124, as well as the 320 pps condition within T2.
396 Additionally, the noise floor in T4 (silence) was significantly smaller for 320 pps compared to the
397 other three pulse rates. No correlation was found between the pulse rate upper limit and the
398 N1P2 amplitude or the ASSR amplitude. However, the ASSR amplitude of the 40 pps condition
399 was correlated with the 160 pps condition.